Food Hydrocolloids 112 (2021) 106285

Contents lists available at ScienceDirect

Food Hydrocolloids

journal homepage: http://www.elsevier.com/locate/foodhyd

Less is more: Limited fractionation yields stronger gels for pea proteins

Remco Kornet [a,b], Justus Veenemans [b], Paul Venema [b,*], Atze Jan van der Goot [c], Marcel Meinders [a,d], Leonard Sagis [b], Erik van der Linden [a,b]

[a] TiFN, P.O. Box 557, 6700, AN Wageningen, the Netherlands
[b] Laboratory of Physics and Physical Chemistry of Foods, Wageningen University, Bornse Weilanden 9, 6708, WG Wageningen, the Netherlands
[c] Laboratory of Food Process Engineering, Bornse Weilanden 9, 6708, WG Wageningen, the Netherlands
[d] Food and Biobased Research, Wageningen University and Research, 6700, AA Wageningen, the Netherlands

ARTICLE INFO

Keywords:
Yellow pea
Aqueous fractionation
Heat-induced gelation
Gel microstructure
Nonlinear rheology

ABSTRACT

Limited fractionation of yellow pea yielded functional protein fractions with higher gelling capacity. Pea protein concentrates were obtained by dispersing flour at unadjusted pH (~6.7) and at pH 8. An additional isoelectric precipitation step resulted in a protein-rich isolate and a protein-poor supernatant. Aqueous solutions of these pea fractions (up to 15 wt %) were heated from 20 to 95 and subsequently cooled to 20 °C, and their viscoelastic response was characterized by small and large amplitude oscillatory shear measurements (SAOS and LAOS, respectively). SAOS rheology showed that the limited fractionated protein concentrates formed significantly firmer gels per mass of protein after cooling, than the more extensively fractionated protein isolate, with elastic moduli of $G' \sim 10^3$ Pa and $G' \sim 10^2$ Pa, respectively. LAOS rheology showed an overall strain softening behaviour for all pea fractions and a transition from elastic to viscous behaviour at smaller strain for the protein isolate. Confocal and electron microscopic images were consistent with those observations, and revealed a more homogeneous network for the limited fractionated samples, and a more heterogenous network for the protein isolate. A number of experiments showed that there are different processing and compositional factors affecting gelling capacity. These are isoelectric precipitation, amount of sugars upon lyophilization and differences in ash content. Furthermore, differences in pre-aggregated state, as found in earlier research, may be partially responsible for the different gelling behaviour. In conclusion, we explain how fractionation affects pea proteins and found that limited fractionation yields pea proteins that form stronger gels.

1. Introduction

In recent years, quite a few studies appeared with a focus on functional behaviour of mildly or limited processed plant proteins (Fuhrmeister & Meuser, 2003; Ntone, Bitter, & Nikiforidis, 2020; Papalamprou, Doxastakis, Biliaderis, & Kiosseoglou, 2009; Sridharan, Meinders, Bitter, & Nikiforidis, 2020). The main reason that mild processing receive considerable interest is that it could contribute to a more sustainable production of foods (van der Goot et al., 2016). Although extensive purification may be beneficial in reducing off-flavours and increasing the general applicability of ingredients, mildly processed fractions often exhibit richer behaviour due to the higher number of components in those fractions, which may lead to a more detailed control of microstructural features. Furthermore, mild or limited processing of plant material may better preserve native properties of biopolymers; less mild processing steps such as heating, pH adjustments and drying can alter the physical state of proteins and (poly)saccharides irreversibly and thus change their functional behaviour. Hence, the functional behaviour of yellow pea fractions will not only depend on the extent of fractionation and its direct consequences for molecular composition, but also on the extent of processing as a determinant of the state of the biopolymers present. The above explains within the field of plant protein food research the interest on functionality as a function of composition and processing history, rather than molecular composition only. Indeed, preventing protein denaturation during fractionation processes can result in better heat-induced gelling properties (Stone, Karalash, Tyler, Warkentin, & Nickerson, 2015; Sun & Arntfield, 2010).

Protein purification can be achieved in different ways, including dry and aqueous fractionation. The latter can be considered as a conventional route (Schutyser, Pelgrom, van der Goot, & Boom, 2015) and has been widely applied. This method has the advantage of achieving high protein purities. It typically involves a solubilization step at elevated pH

* Corresponding author.
E-mail address: paul.venema@wur.nl (P. Venema).

https://doi.org/10.1016/j.foodhyd.2020.106285
Received 23 April 2020; Received in revised form 26 August 2020; Accepted 26 August 2020
Available online 28 August 2020
0268-005X/© 2020 The Authors. Published by Elsevier Ltd. This is an open access article under the CC BY-NC-ND license (http://creativecommons.org/licenses/by-nc-nd/4.0/).

(8–10), separation of the soluble and insoluble part and subsequent isoelectric precipitation (pH 4–5) of the formerly soluble proteins and spray or freeze drying (Berghout, Venema, Boom, & van der Goot, 2015; Makri, Papalamprou, & Doxastakis, 2005; Puppo et al., 2011). At the same time, different studies have reported the pH sensitivity of pea and soy proteins on their functionality. Shifting the pH-value to acidic pH (<3.5) or alkaline pH (>9) were found to induce irreversible modification of the proteins, leading to e.g. reduced solubility (Gueguen, Chevalier, And, & Schaeffer, 1988; Jiang, Chen, & Xiong, 2009). Furthermore, it was found that precipitation of pea proteins at pH 4.5 resulted in a 20% reduction of solubility and the formation of both soluble and insoluble aggregates (Kornet et al., 2020). The solubility of commercial pea protein isolates (PPI) is substantially lower, with reported solubility values ranging from 20 to 60% at pH 7 (Lam, Can Karaca, Tyler, & Nickerson, 2016; Shand, Ya, Pietrasik, & Wanasundara, 2007; Taherian et al., 2011). The proteins in those isolates are often completely denatured, probably as a result of pH changes combined with elevated temperatures upon extraction or drying.

Thermal stability of proteins is an important functional property in food applications (e.g. high protein drinks and food gels) and there have been several studies on the gelation behaviour of pea proteins. It was found that native pea globulins mostly aggregate through hydrophobic interaction upon heating, and hydrogen bonding upon cooling, and that disulphide bonding does not play a major role (Francesca Elizabeth O'Kane, 2004; Francesca E O'Kane, Happe, Vereijken, Gruppen, & van Boekel, 2004; Sun & Arntfield, 2012). Other studies found that the protein extraction process influences the gel firmness of PPI and that commercial PPI generally perform poorer compared to lab-extracted PPI (Sun & Arntfield, 2011). Despite these studies, a gap exists on the effects of the different steps in a conventional aqueous extraction on the gelling properties of yellow pea protein, allowing to optimize the intensity of fractionation and according gel properties. Here we will address this gap for yellow pea, building further on our findings in previous research on the compositional and physicochemical changes upon aqueous fractionation of yellow pea (Kornet et al., 2020).

In this study we examine the effect of aqueous fractionation on the thermal stability and gelling behaviour of the resulting yellow pea. The viscoelastic behaviour during and after heating is studied and related to

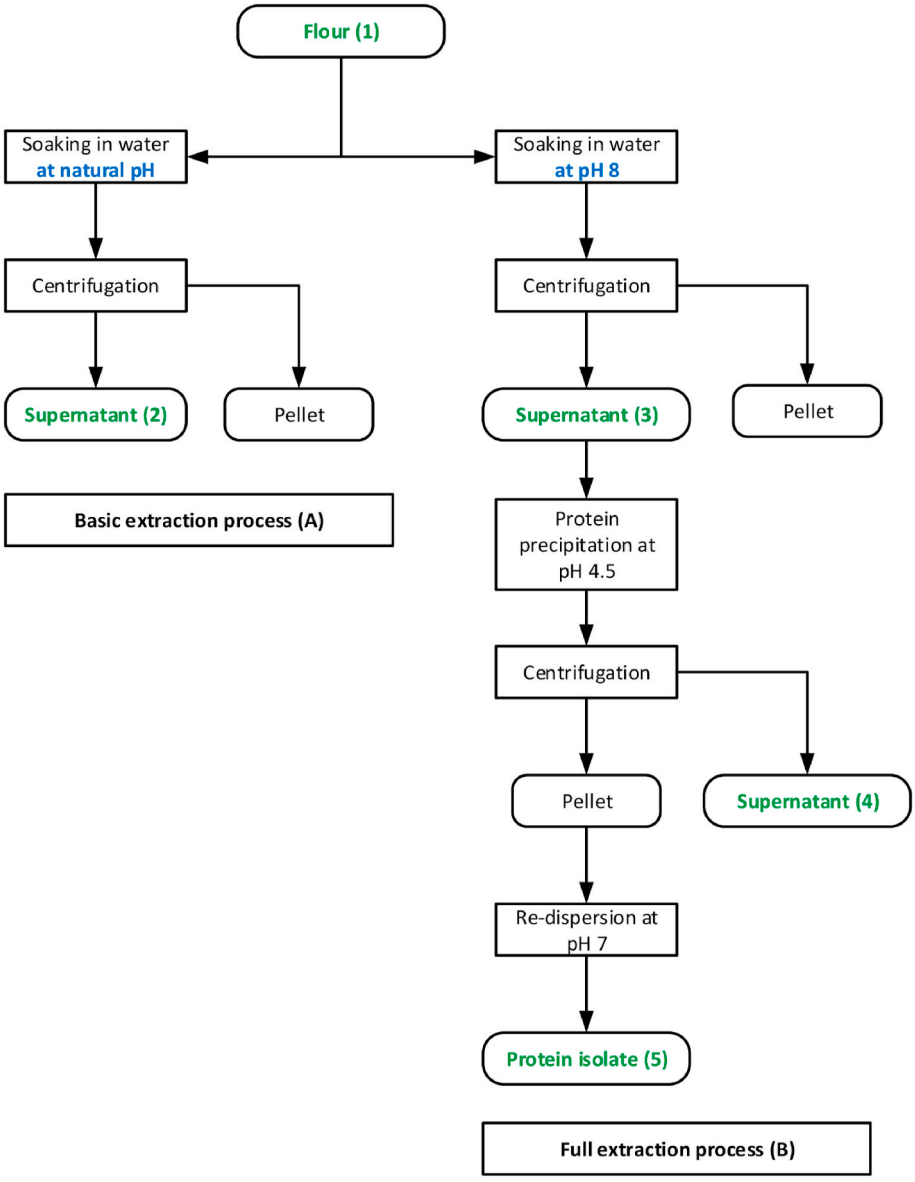

Fig. 1. Schematic overview of the basic (A) and full extraction process (B) for yellow pea (Kornet et al., 2020). (For interpretation of the references to colour in this figure legend, the reader is referred to the Web version of this article.)

the microstructure of the obtained gels. These measurements were complemented with rheological measurements and chemical analyses to find explanations for differences in gelling capacity upon more extensive fractionation.

2. Materials and methods

2.1. Materials

Yellow pea (*Pisum sativum* L.) seeds were obtained from Alimex Europe BV (Sint Kruis, The Netherlands). All chemicals and reagents were obtained from Merck (Darmstadt, Germany) and were of analytical grade.

2.2. Methods

2.2.1. Yellow pea extraction process

Yellow pea protein fractions varying from limited to extensively fractionated, were obtained according to the method described earlier by Kornet et al. (2020). Two aqueous purification processes were used (Fig. 1). In both processes flour was dispersed in deionized water and pH was adjusted by adding 1 M NaOH or HCl solutions. A limited fractionation process (A) included yellow pea flour dispersion at unadjusted pH under mild agitation for 2 h, and subsequent centrifugation at 10000g for 30 min. The yellow pea flour and supernatant were labelled fraction 1 and 2 respectively. The second, more extensive fractionation process (B) also started with flour dispersion under mild agitation for 2 h, but the pH was adjusted to pH 8 beforehand. The dispersion was centrifuged (10000g, 30 min) and the supernatant was labelled fraction 3. This fraction was further purified by isoelectric precipitation at pH 4.5 and subsequently centrifuged (10000g, 30 min). The obtained supernatant was labelled fraction 4 and the pellet was re-dispersed at pH 7 and labelled fraction 5. All steps in the fractionation processes, including centrifugation, were conducted at room temperature and the obtained fractions were frozen and lyophilized with an Alpha 2–4 LD plus freeze-dryer (Christ, Osterode am Harz, Germany) and then stored at −18 °C. Protein content was determined by a Flash EA 1112 series Dumas (Interscience, Breda, The Netherlands) using a nitrogen conversion factor of 5.7. In Kornet et al. (2020) the effect of the fractionation processes on composition and protein recovery was studied. The results from this study are shown in Table 1, where the composition of fraction 1 is identical to that of the yellow pea seed. Fraction 1 is the pea flour and can be considered a starch-rich fraction, fractions 2 and 3 protein concentrates, fraction 4 a protein-poor side stream and fraction 5 a protein isolate.

2.2.2. Preparation of gels

The dried fractions were dissolved in deionized water at a concentration of 15 wt % at room temperature, under mild agitation with a magnetic stirrer for 2 h. Within the first hour the pH was adjusted to 7, using 1 M NaOH or HCl solutions. The solutions were transferred to 15 mL syringes, with paraffin applied on the inside, and closed with a syringe cap. The samples were heated by bringing the syringes to a water bath set to 95 °C and keeping them at this temperature for 15 min. After heat treatment, the samples were cooled to room temperature. The samples were taken out of the syringes gently and cut into small slices with a height of 2 mm. These gels were used for microscopy, as described later.

2.2.3. Hydrophobicity

Hydrophobicity was determined using 8-anilino-1-naphthalenesulfonic acid (ANSA) as a fluorescent probe, according to the method of Kato and Nakai (1980) (Kato & Nakai, 1980). The yellow pea fractions were dissolved and pH was adjusted to 7. The stock solution was diluted five times to protein concentrations within a range of 0.03–0.16 wt %. ANSA reagent (8 mM) was added to the sample in concentrations of 10 μl/3 mL sample. The samples were stored in the dark for 1 h to allow ANSA to bind to the hydrophobic sites on the surface of the proteins. Subsequently, fluorescence intensity was measured with a luminescence spectrometer LS50B (PerkinElmer, Waltham, United States) at wavelengths of 390 nm (excitation) and 470 nm (emission). The measured values were corrected for the intrinsic fluorescence of all dilutions before addition of ANSA. All samples were measured in duplicate. The initial slope of fluorescence intensity versus protein concentration was used as an index for hydrophobicity.

2.2.4. Sulfhydryl content

The number of exposed sulfhydryl groups was determined using the Ellman protocol (Creighton, 1997; Ellman, 1959; Wierenga, Kosters, Egmond, Voragen, & de Jongh, 2006). The Ellman's reagent or 2-nitro-5-mercaptobenzoic acid (DTNB) reacts with free thiol groups of the protein and is used as a reagent for spectrophotometric analysis. A 0.2% DNTB solution was prepared by dissolving DNTB in a 0.1 M sodium phosphate buffer pH 8. A protein stock solution was prepared with 5 mg protein in 1 mL 0.1 M sodium phosphate pH 8.0 buffer. From this stock solution 250 μl was taken and 10 times diluted by 0.1 M sodium phosphate pH 8.0 buffer. To this dilution 50 μl of the Ellman's reagent solution was added. Also, a blank sample without protein was prepared. The solutions were subsequently incubated for 15 min. After incubation, the absorbance was measured with a Shimadzu UV1800 spectrophotometer (Shimadzu, Kyoto, Japan) at a wavelength of 412 nm. All samples were measured in duplicate.

Since literature values for the extinction coefficient of the NTB anion vary within a wide range, a calibration curve with cysteine as calibration standard was made. For this calibration curve, a dilution series was prepared from a 0.5 mM L-cysteine HCl monohydrate (Sigma, C-4820) in 0.001 N HCl stock solution. The calibration curve provided an extinction coefficient for the reduced conjugate of 13,691 M^{-1} cm^{-1} ($R^2 = 0.998$). The absorbance value for the blank was subtracted from all absorbance values to calculate the net absorbance value.

2.2.5. Electrophoretic mobility

The electrophoretic mobility, a measure for the ζ-potential, of the yellow pea fractions was determined with a ZS Nanosizer (Malvern, Worcestershire, United Kingdom). The sample was dissolved in 0.1 M phosphate buffer pH 7 to obtain a 0.1 wt % solution. This solution was

Table 1
Dry matter composition of the yellow pea fractions (Kornet et al., 2020). The recovery is defined as the recovered amount of protein divided over the initial protein content in the flour. Standard deviations are shown between brackets.

	Recovery	Protein content	Total carbohydrate content	Starch or starch derivative content	Ash content
	(%)	g/100 g dry matter			
Fraction 1	100	18.8 $^{\pm 0.2}$	59.8 $^{\pm 2.1}$	48.7 $^{\pm 1.7}$	3.7 $^{\pm 0.3}$
Fraction 2	53	46.3 $^{\pm 0.9}$	30.9 $^{\pm 0.3}$	4.1 $^{\pm 0.3}$	13.2 $^{\pm 0.8}$
Fraction 3	70	51.4 $^{\pm 0.8}$	23.6 $^{\pm 0.1}$	3.5 $^{\pm 0.2}$	11.8 $^{\pm 0.3}$
Fraction 4	17	21.1 $^{\pm 0.2}$	34.8 $^{\pm 2.2}$	6.0 $^{\pm 0.0}$	21.1 $^{\pm 0.5}$
Fraction 5	44	87.3 $^{\pm 1.0}$	3.4 $^{\pm 0.6}$	0.3 $^{\pm 0.1}$	6.0 $^{\pm 0.0}$

transferred to a capillary zeta cell and the electrophoretic mobility was determined using Phase Analysis Light Scattering (PALS). The phase is shifted in proportion to the particles velocity. This phase shift is determined by comparing the phase of the light scattered by the particles with the phase of a reference beam. The electrophoretic mobility, and the according ζ-potential, is generated by summing the phase shifts during the Fast Field Reversal (FFR) part of the measurement.

2.2.6. Differential scanning calorimetry (DSC)

The protein denaturation and starch gelatinization temperatures in the pea fractions were determined using DSC. The samples were prepared by dissolving 10 (w/v) protein in deionized water for 2 h at pH 7. This solution was transferred to TA high volume pans in quantities of 20–30 mL. The pans were closed and measured with a TA Q200 Differential Scanning Calorimeter (TA Instruments, Etten-Leur, The Netherlands), in a range of 20 °C–120 °C with incrementing temperature of 5 °C/min. All samples were measured in triplicate.

2.2.7. Small amplitude oscillatory shear (SAOS)

The dried fractions were dissolved in deionized water at a concentration of 15 wt % drat room temperature, under mild agitation with a magnetic stirrer for 2 h. Within the first hour the pH was adjusted to 7, using NaOH or HCl. For certain experiments the samples were standardized on 10 wt % protein with varying dry matter. The amount of dry matter was calculated based on the protein content of the pea fractions.

The linear viscoelastic properties of the samples were evaluated with SAOS. The samples were measured with an MCR302 rheometer (Anton Paar, Graz, Austria) combined with a sand-blasted CC-17 concentric cylinder geometry. Gelling occurred within the cylinder and to prevent solvent evaporation during heating, a solvent trap was placed on top of the cylinder. The samples were sequentially exposed to a temperature, frequency and strain sweep. Upon thermal treatment the temperature increased from 20 to 95 °C at a rate of 3 °C/min. The samples were kept at 95 °C for 10 min before cooling back to 20 °C at a rate of 3 °C/min. Subsequently, the gels were subjected to a frequency sweep from 0.01 to 10 Hz (at a strain of 1%). The storage (G') and loss modulus (G'') dependency on temperature and frequency was recorded.

The pea fractions are compared on different parameters, including gelling capacity and gel strength. The gelling capacity is defined as the capacity per mass of protein to increase the G' upon thermal treatment. Gel strength is defined as the elastic modulus after heat treatment. The end of the linear viscoelastic regime is defined as the strain at which the elastic modulus has decreased to 90% of its plateau value.

2.2.8. Large amplitude oscillatory shear (LAOS)

After the SAOS measurements, a strain sweep was applied to determine the elastic and viscous behaviour of the 15 wt % yellow pea fraction gels in the nonlinear regime. LAOS was a continuation of SAOS so the same geometry and gels were used. The gels were studied at a logarithmically increasing strain range of 0.1–1000% in 10 min to collect 80 data points. The temperature and frequency were kept constant at 20 °C and 1 Hz. The oscillating strain, stress, and shear rate signals were recorded for an imposed sinusoidal strain and used to construct Lissajous plots. The intra-cycle stiffening behaviour (S factor) and intra-cycle thickening behaviour (T factor) were determined as described by Ewoldt, Hosoi, and McKinley (2008):

$$S = \frac{G'_L - G'_M}{G'_L} \tag{1}$$

$$T = \frac{\eta'_L - \eta'_M}{\eta'_L} \tag{2}$$

where, G'_L and G'_M are the shear elastic modulus at maximum strain (i.e. the secant modulus) and the tangential modulus at zero strain, respectively. The viscosities η'_L and η'_M are the viscosity at maximum shear rate and tangential viscosity at zero shear rate respectively. The S- and T-factors were automatically calculated using the Anton Paar Rheocompass Software.

Stress decomposition was done manually to visualise the elastic and viscous contribution to the measured stress response. This method originates from orthogonal stress decomposition (Cho, Hyun, Ahn, & Lee, 2005), using symmetry arguments to decompose the generic nonlinear stress response into a superposition of an elastic and viscous stress, σ' and σ''. The decomposition is based on the idea that the elastic stress should exhibit odd symmetry with respect to $x = \gamma / \gamma_0$ and even symmetry with respect to the $y = \dot{\gamma} / \dot{\gamma}_0$ and for the viscous stress vice versa. (Ewoldt et al., 2008). The stress and viscous contribution was determined from:

$$\sigma' = \frac{\sigma(\gamma, \dot{\gamma}) - \sigma(-\gamma, \dot{\gamma})}{2} \tag{3}$$

$$\sigma'' = \frac{\sigma(\gamma, \dot{\gamma}) - \sigma(\gamma, -\dot{\gamma})}{2} \tag{4}$$

2.2.9. Confocal laser scanning microscopy (CLSM)

The proteins in the gel were stained in a 0.002% fluorescent dye Rhodamine B solution for 2 h and washed with water twice for 2 h. The microstructures were visualized using a Leica SP8X-SMD confocal laser scanning microscope (Leica, Amsterdam, The Netherlands), coupled with a white light laser. A dry objective (10x, 0.40) and water immersion objectives (20x, 0.70 and 63x, 1.20) were used for magnification. The laser excitation wavelength and the filter emission wavelength were 543 and 580 nm respectively.

2.2.10. Cryo-scanning electron microscopy (CryoSEM)

CryoSEM was used to visualise the microstructure of gelled fraction 1 and 5. A small piece of the gel was frozen with liquid ethane and transferred to a sealed cryo-chamber for planing with a Leica EM FC7 microtome (Leica, Eindhoven, the Netherlands). The sample was pre-planed with a glass knife and planing was finalized with a diamond knife to ensure a smooth surface. Subsequently, the sample was sublimated under vacuum and sputter coated with platinum. It was then transferred to the SEM chamber (Jeol, Nieuw-Vennep, The Netherlands) and cooled to −110 °C. The surface of the samples was scanned with a focussed beam of electrons to produce images of different regions in the sample. Energy-dispersive X-ray Spectroscopy (EDS) was used to obtain elemental maps of some of these regions.

2.2.11. Additional rheological experiments to test specific hypotheses

Additional rheological tests were performed to test different hypothesis regarding observed differences between pea fractions. The results of these tests are described in section 3.3 and here the methods are briefly discussed. In all cases, dispersion of 15 wt % dry matter in deionized water were made and the pH was adjusted to 7 with NaOH or HCl. All rheological measurements were performed as described in section 2.2.7.

To test the effects of ionic strength an estimation of the initial ionic strength was made based on the ash content and verified with conductivity measurements. For the calculation it was assumed that all salts was present as sodium chloride, as this is the most abundant salt as a consequence of pH adjustments with NaOH and HCl in the fractionation process. Sodium chloride was added to dispersions in concentrations of 20 and 200 mM NaCl.

The impact of composition was tested by reversing the fractionation process Fractions 4 and 5 were mixed in a ratio of 54 : 46 to obtain a similar composition and the same protein content as fraction 3. The mixture was dispersed and measured the same way as all other samples.

The effects of isoelectric precipitation and pH changes were also determined by rheology measurements. The isoelectric precipitated fraction 5 was compared to fraction 2 that was further purified by

dialysis with a 12–14 kDa cut-off size. The dialysis tubes were placed in a bucket of demineralized water at 4 °C and dialysis was finished when the conductivity of the surrounding water remained constant. The dialysed fraction 2 was freeze dried and measured the same way as the other samples. For the experiments showing the effect of pH shifts, a separate batch of fraction 2 was made of which half was taken and exposed to 2 h stirring at pH 4.5 and 2 subsequent hours at pH 7. To compensate for the added salt after the pH adjustments, the conductivity between the two halves was made constant by adding sodium chloride to the part that was not exposed to pH changes. Both fractions were freeze dried afterwards.

The contribution of thiol groups to the gel formation was studied by adding a thiol blocking agent. For this experiment, 15 wt % pea fractions were dissolved in a 20 mM N-Ethylmaleimide (NEM) solution, the pH was adjusted to 7, and the dispersions were measured as described in section 2.2.7.

2.2.12. Statistical analysis

All measurements were performed at least in duplicate. The mean values and standard deviations were calculated and used as a measure of error. Claims regarding significant effects were supported by ANOVA analysis, followed by Tukey's post hoc test. Significance was defined as $P < 0.05$.

3. Results and discussion

This results and discussion section starts with the thermal properties and gelation behaviour of the pea fractions. Then their according microstructures are discussed and finally different experiments are described to explain the differences between limited fractionated and extensively fractionated pea fractions.

3.1. Denaturation and viscoelastic behaviour upon heating

3.1.1. Differential scanning calorimetry

To determine the effect of fractionation processes on protein denaturation, the pea fractions were exposed to a thermal treatment and the heat flow was recorded. The peak denaturation temperatures and heat enthalpies are shown in Table 2. It was found that the proteins remained at least partially native in all pea fractions. Fraction 1 shows starch gelatinization and protein denaturation in the different fractions with their standard deviations. Starch gelatinization occurred at 67.1 °C (±0.24 °C). The globulins in the protein-enriched fractions 2,3 and 5 denatured at 83.8 °C (±0.41 °C). The albumin-enriched fraction 4 showed a denaturation peak at 88.1 °C (±0.19 °C). The temperatures for pea starch gelatinization and globulin denaturation are in line with what has been reported in literature (Biliaderis, Maurice, & Vose, 1980; Mession, Sok, Assifaoui, & Saurel, 2013). In contrast to the denaturation temperatures reported in literature, there is quite some variation in the reported heat enthalpies of pea protein. Shand et al. (2007) reported ΔH values for native pea protein isolate (81% protein) ranging from 0.725 to 0.922 J/g, depending on the salt concentration and at a pH of ~6.5 (Shand et al., 2007). Another study reported values of 15.81 and 17.84 J/g protein at 0 M and 0.3 M NaCl respectively and at a pH of around 5.7 (Sun et al., 2010). The ΔH reported in Table 2 do not vary to a great extent and range between 5.5 and 8.9 J/g. Factors that influence the denaturation temperate and heat enthalpy include moisture content, heating rate and presence of salts and sugars. In this study there is significant variation in dry matter and sugar content, which could be an important factor that explains the differences in heat enthalpy between the protein-enriched fractions 2, 3 and 5.

Table 2
Onset and peak denaturation temperatures (°C) and denaturation enthalpies (J/g) of the pea fractions at pH 7. All standard deviations are smaller than 1 °C or 1 J/g.

Pea fraction	Denaturation onset (°C)	Peak denaturation (°C)	Heat Enthalpy (J/g)
Fraction 1	59.3	67.1	–
Fraction 2	73.6	83.7	5.5
Fraction 3	77.4	84.3	3.6
Fraction 4	81.8	88.1	3.3
Fraction 5	73.8	83.6	8.9

3.1.2. Small amplitude oscillatory shear (SAOS)

The gelation behaviour of the yellow pea fractions upon and after thermal treatment was studied by SAOS, shown in Fig. 2 and Fig. 3. The pea fractions 1–5 were standardized on 15 wt % dry matter to study the gelling behaviour of the overall pea fractions. To better compare the protein-enriched fractions 2, 3 and 5 additional experiments were conducted in which those fractions were standardized on 10 wt % protein.

3.1.2.1. Gelation behaviour of dry matter standardized dispersions. The gelation behaviour of the yellow pea fractions upon and after thermal treatment was studied by SAOS, shown in Fig. 2. The maximum temperature during the thermal treatment was higher than the denaturation temperature of the globular pea proteins. Also the onset of gelation is consistent with Table 2. Fig. 2 shows an abrupt increase of the elastic moduli for the starch-rich fraction 1 at around 70 °C and the protein-rich fractions 2,3 and 5 upon heating from ~75 to 95 °C. The steep increase in G' observed in fraction 1 is expected to mainly originate from water absorption and swelling of the starch granules, since starch is the major constituent. The subsequent decrease in G' could be due to loss of crystallinity, subsequent uncoiling, dissociation of double helices and leaching of amylose in the continuous phase (Ratnayake, Hoover, & Warkentin, 2002). The gelling of the limited processed fractions 2 and 3 (46 and 51 wt % protein resp.) is caused by protein denaturation, as earlier research showed that the carbohydrate impurities are only present in the form of small sugar molecules (Kornet et al., 2020). Protein denaturation results in a gradual increase in G' at around 75 °C. Gelling of pea globulins was reported to be mainly based on hydrophobic and electrostatic interactions (Sun et al., 2012). Upon heating, the hydrophobic interior of the proteins become exposed, resulting in hydrophobic interactions and subsequent network formation. During the holding time at 95 °C, G' increases more for these limited processed fractions 2 and 3 than for fraction 1. The decrease afterwards as observed in fraction 1, is virtually absent for fractions 2 and 3. Upon cooling the gel firmness increases further. The protein-poor fraction 4 (21.1 wt % protein), which is the supernatant after a protein precipitation step, shows limited gel formation. The G' (T(t)) and G'' (T(t)) of the extensively processed fraction 5 (87 wt % protein) shows a similar behaviour as that of fraction 2 and 3, but with a reduced gelling capacity, as indicated by the less pronounced G' increase upon heating and cooling. Moreover, the limited processed fractions 2 and 3 (~50 wt % protein) form firmer gels on protein weight basis than the further fractionated fraction 5. Explanations for this reduced gelling capacity of the protein in fraction 5 are discussed in section 3.3. Table 3 shows the G' and tan δ of fraction 1–5 after heat treatment. It was found that the G'-values of fraction 2, 3 and 5 are of the same order of magnitude (10^3 Pa), despite of the substantial differences in protein content between fraction 2 or 3 and fraction 5. The tan δ values of the studied yellow pea fractions were all below 0.25, indicating solid-like behaviour after heat treatment. Furthermore, it is noted that fraction 2 has the lowest tan δ of 0.04, indicating a more solid-like response. Overall the pea fractions showed tan δ values that correspond with weak elastic gels. Hence the non-linear regime of the gelled fractions was studied by applying oscillatory deformation with a rheometer. Using the same concentrations as used for SAOS measurements, the gels were not firm enough to cut uniform pieces that are required for compressional deformation with a texture analyser.

The G' and G'' dependencies on frequency were determined through a frequency sweep in a range of 0.1–10 Hz. For all fractions, G' and G''

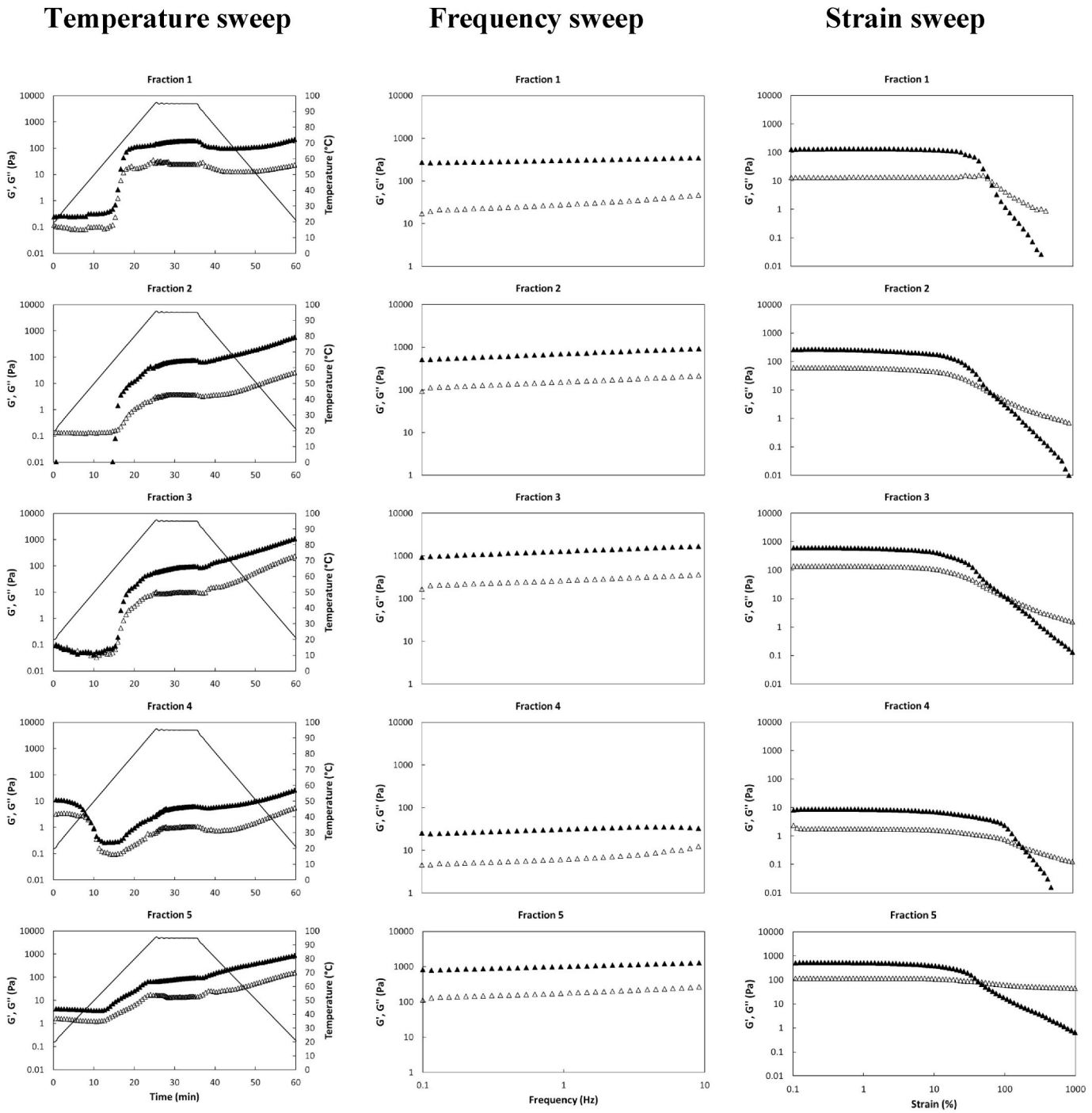

Fig. 2. Temperature (20–95 °C, f = 1 Hz, γ = 1%), frequency (0.1–10 Hz) and strain sweeps (0.1–1000%) sequentially applied on yellow pea fractions 1–5 standardized on dry matter (15 wt % in water adjusted to pH 7) at 20 °C. *G'*: closed symbols, *G''*: open symbols, Temperature: solid line. (For interpretation of the references to colour in this figure legend, the reader is referred to the Web version of this article.)

remained fairly constant over this frequency range, indicating that G' and G'' are only slightly dependent on frequency in this range. Although generally a stronger dependency on frequency is observed for weak gels, a similar observation was seen by Sun et al. (2010). For commercial and salt-extracted pea protein isolate only a small increase of G' was observed over a range of 0–10 Hz, despite of tan δ values of 0.8 and 0.2 respectively, indicating a weak gel. The almost flat line with increasing frequency could indicate the presence of a broad relaxation spectrum that is typical for a disordered system. Generally colloidal gels in a low viscosity solvents show little to no frequency dependency (Bandyopadhyay, Liang, Harden, & Leheny, 2006). The elastic moduli at f < 0.1 Hz could not be studied due to the low signal to noise ratio of the rheometer in these regions. After heat-induced gelation, the length of the linear viscoelastic (LVE) regime was studied by a strain sweep at constant frequency (Fig. 2). The end the LVE regime was expressed as the critical strain (γ_c), shown in Table 3. The starch-rich fraction 1 appeared slightly more tensile, whereas the length of the LVE regimes of fractions 2, 3 and 5 were rather similar. A more detailed analysis on the transition from elastic to viscous behaviour is discussed in section 3.1.3.

The similar elastic moduli of the gels from fractions 2, 3 and 5, despite their differences in protein purity, indicate a higher gelling capacity (defined here as the capacity per mass of protein to increase the

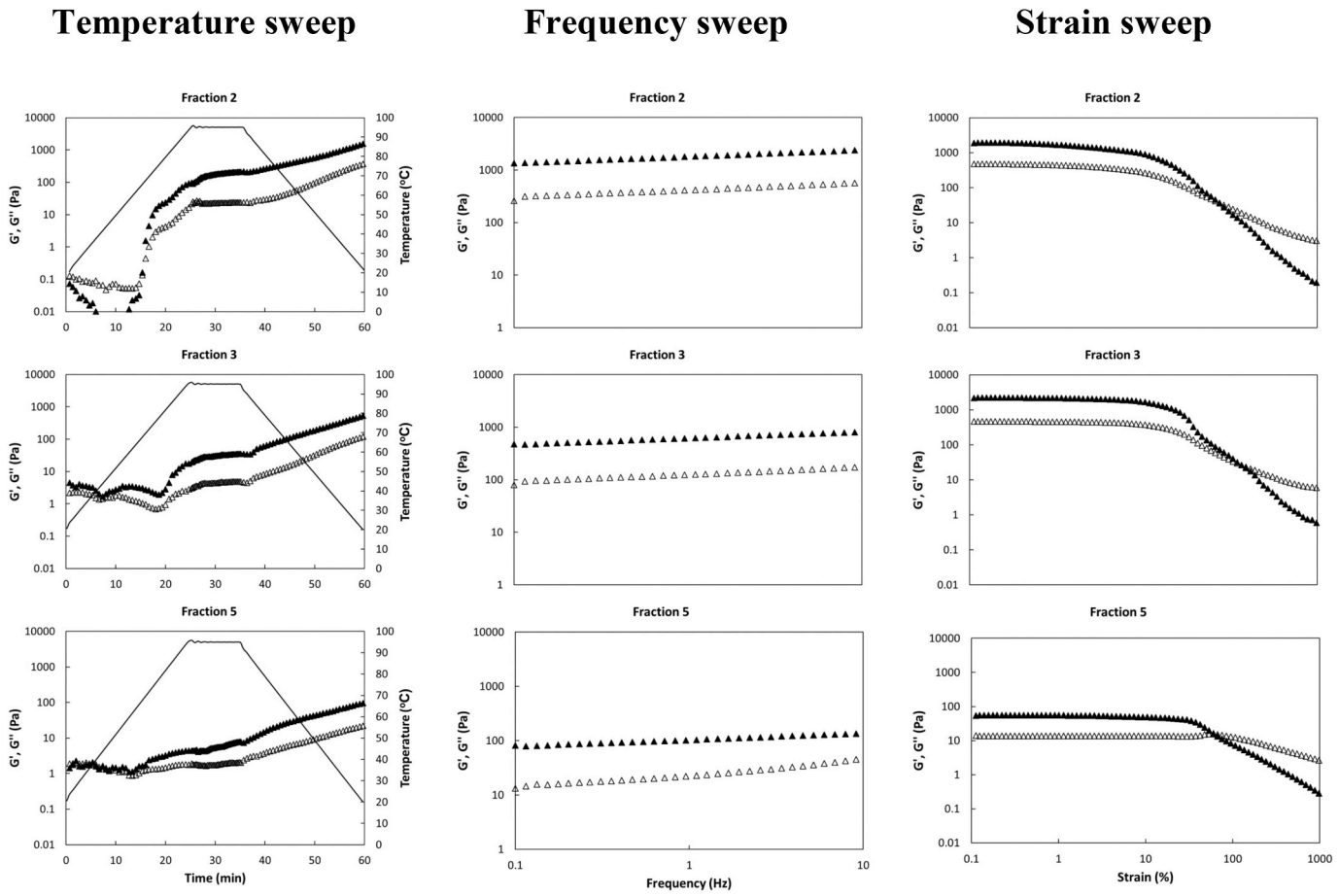

Fig. 3. Temperature, frequency and strain sweeps sequentially applied on yellow pea fractions 2, 3 and 5 standardized on protein content (10 wt % in water adjusted to pH 7). *G'*: closed symbols, *G''*: open symbols. Temperature: solid line. (For interpretation of the references to colour in this figure legend, the reader is referred to the Web version of this article.)

Table 3
Average elastic moduli (*G'*), loss factors (tan δ) and critical strains (%) of the gelled pea fractions. The elastic moduli and loss factor correspond with the values of the last data point from the temperature sweeps and the critical strains are determined from the temperature sweeps. All results presented here originate from one batch of pea fractions that was used for this study. Standard deviations are shown in superscript.

	Fraction 1	Fraction 2	Fraction 3	Fraction 4	Fraction 5
Rheological properties of dry matter standardized gels					
G' (Pa)	229 $^{\pm 103}$	623 $^{\pm 127}$	1174 $^{\pm 185}$	28 $^{\pm 11}$	921 $^{\pm 4.9}$
Tan δ	0.11 $^{\pm 0.02}$	0.04 $^{\pm 0.00}$	0.21 $^{\pm 0.00}$	0.21 $^{\pm 0.02}$	0.18 $^{\pm 0.01}$
γ_c (%)	11.2 $^{\pm 6.3}$	3.32 $^{\pm 1.8}$	4.95 $^{\pm 3.4}$	2.43 $^{\pm 0.2}$	7.02 $^{\pm 4.8}$
Rheological properties of protein standardized gels					
G' (Pa)	–	1658 $^{\pm 315}$	573 $^{\pm 175}$	–	97 $^{\pm 15.2}$
Tan δ	–	0.24 $^{\pm 0.00}$	0.21 $^{\pm 0.00}$	–	0.23 $^{\pm 0.01}$
γ_c (%)	–	1.12 $^{\pm 0.45}$	4.95 $^{\pm 1.22}$	–	14.5 $^{\pm 5.80}$

G' upon thermal treatment). This higher gelling capacity is discussed further in the next section, where fractions 2, 3 and 5 are standardized on protein content.

3.1.2.2. Gelation behaviour of protein standardized dispersions. As the main impurities of fraction 2–5 are sugars, the contribution of protein on the gelling capacity was studied further by standardizing fractions 2, 3 and 5 on protein content. For fractions 1 and 4 it was not possible to standardize on 10 wt % protein, since this would require dispersion of 50 wt % dry matter because of lower protein purities. Results are depicted in Fig. 3 showing the G', G'' dependency on temperature, frequency and strain of fraction 2, 3 and 5 that are standardized on 10 wt % protein. The corresponding dry matter concentrations were 21.6, 19.5 and 11.5 wt % respectively.

The left panels of Fig. 3 show the results of the temperature sweeps. The initial elastic modulus G' was higher for the fractions that were more extensively fractionated, while the eventual G'-values after gelation were higher for the fractions that were limited fractionated. Fraction 5 has the highest initial elastic modulus and fraction 2 has the highest final elastic modulus. The first phenomenon has been described earlier (Kornet et al. (2020)), where pea protein was found to possess high intrinsic viscosity. The higher gelling capacity of the limited processed fractions at equal protein content of 10 wt % indicates that gel strength is not only related to protein quantity.

Fig. 3 shows that the protein-standardized fractions showed G' to be independent of frequency in this range. From the strain sweeps (Fig. 3), it was found that the length of the LVE regime correlated inversely with the gel strength. Table 3 shows that fraction 2 had the shortest linear viscoelastic (LVE) regime (γ_c = 1.12%), whereas fraction 5 had the largest maximum linear strain (γ_c = 14.5%). The decline of G' at lower strain is explained by disruption of the gel network structure, resulting in more fluid-like behaviour. Fraction 5 visually appeared to be of paste-like character, which is presumably due to non-connected protein aggregates, as further discussed in section 3.3. For paste-like materials such as fraction 5, increasing strain may result in deformation and displacement of protein aggregates or other components, rather than disruption of a network. Another study that compared two types of waxy rice starch gels also showed that a waxy rice starch, which appears more paste-like (G' ~ 30 Pa), was significantly more stretchable than the

firmer debranched waxy rice starch gel (Precha-Atsawanan, Uttapap, & Sagis, 2018). At small deformations and equal protein concentrations, the limited processed fractions resulted in firmer gels, but the extensively processed fraction 5 was able to withstand larger deformation.

3.1.3. *Large amplitude oscillatory shear (LAOS)*

LAOS measurements were performed to further characterize gel properties of the 15 wt % (dry matter based) gels by understanding their rheological behaviour beyond the LVE regime. From the LAOS data Lissajous plots were constructed with stress versus strain and stress versus strain rate (Fig. 4a and b, respectively). Also, the elastic and viscous stress contributions were plotted (black solid lines). At a strain of 1%, Fig. 4a shows elliptical shapes indicating predominantly elastic or linear viscoelastic behaviour, particularly for the starch-based fraction 1. The Lissajous plot of fraction 4 show some irregularities due to its low *G'* and resulting machine inertia effects. At 26% strain, deflections of the elliptical shape at maximum deformation indicate a mild intracycle strain stiffening behaviour. This intracycle stiffening behaviour is most pronounced in fraction 2 and 3, and to lesser extent in fraction 1. However, the apparent stiffening effect is small, and as we will see later in Fig. 5, the behaviour of these samples in the overall strain sweep, shown earlier in Fig. 2, is mildly strain softening. At a deformation of 170%, fraction 3 gave a Lissajous plot with an almost rhomboidal shape. This implies that, the initial response is highly elastic at the start of a cycle, at $\gamma = -1.7$. When γ increases, abrupt yielding of the gel structure occurs (as indicated by the sudden change in slope of the plot). In the subsequent part of the cycle, the elastic contribution to the stress is nearly zero, and the response is predominantly viscous. At the end of this part of the cycle, the structure recovers, which results in an increase of the elastic contribution and an *apparent* stiffening behaviour. At even higher strain ($\geq$170%) fraction 2 and 3 again show cyclic yielding and recovery, but now clear oscillations are visible in the rhomboidal shape. It could be argued that such behaviour is caused by inertia effects of the measuring device, as seen by Birbaum, Haavisto, Koponen, Windhab, and Fischer (2016) for interfacial rheology. Oscillations were observed at higher strains and they appeared to be highly reproducible, also when particles on the interface were absent (Birbaum et al., 2016). The oscillations in Fig. 4a are more regular however, and also correspond with intersections in the viscous Lissajous curves shown in Fig. 4b. Such self-intersections were also seen for tomato paste and wheat flour dough (Duvarci, Yazar, & Kokini, 2017; Yazar, Duvarci, Tavman, & Kokini, 2017) and can emerge from a timescale for restructuring that is shorter than the oscillatory deformation time scale. Hence the Lissajous curves for fractions 2 and 3 at higher strain probably reflect material properties. The type of plots are typical when the higher harmonics in the response have a phase close to $\pi/2$, so after yielding the response is almost completely viscous. This is also clear from the elastic contribution to the stress, which is nearly zero except when γ is very close to $\pm\gamma_0$. Fraction 5 did not show yielding at larger deformations and the transition to flow occurred at smaller strain, which is also indicated by the lack of elastic contribution at a strain of $\geq$170%. (Ewoldt et al., 2008; Fuongfuchat et al., 2012; Precha-Atsawanan et al., 2018). For fraction 1 and 4 the LAOS data at largest strain (846%) could not be measured. Overall, it is noted that the transitions from elastic to viscous occur at smaller strain for the extensively processed fraction 5 than the limited processed fraction 2 and 3. For fraction 5 the Lissajous plot is already circularly shaped at a deformation of 170% (Fig. 4a), indicating predominantly viscous behaviour.

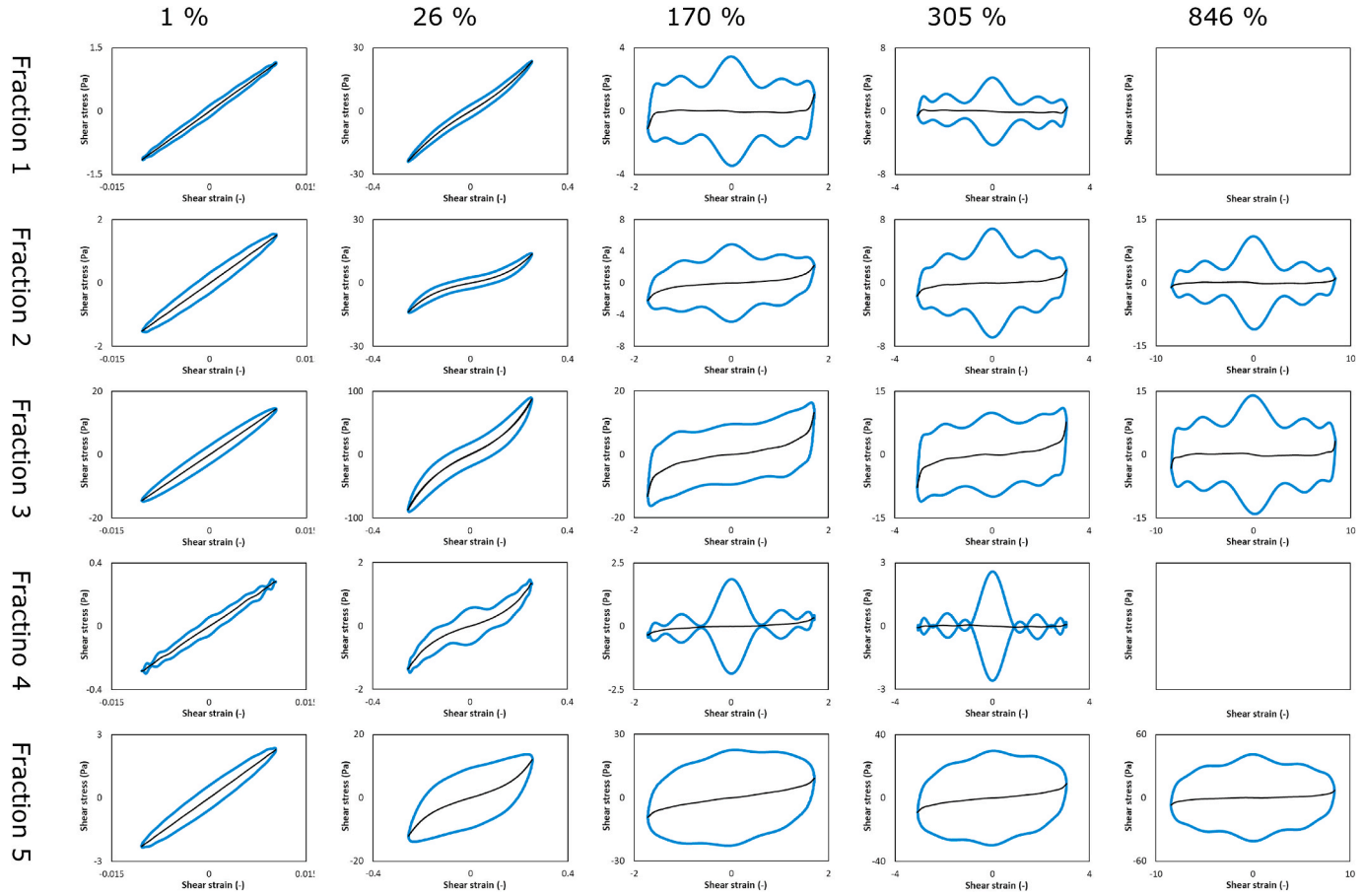

Fig. 4a. Lissajous plots of stress versus strain (τ, γ) at strains of 1, 26, 170, 305 and 846% for; (1–5) gelled fraction 1–5 (15 wt% d.m., pH 7). The black line represents the elastic stress contribution.

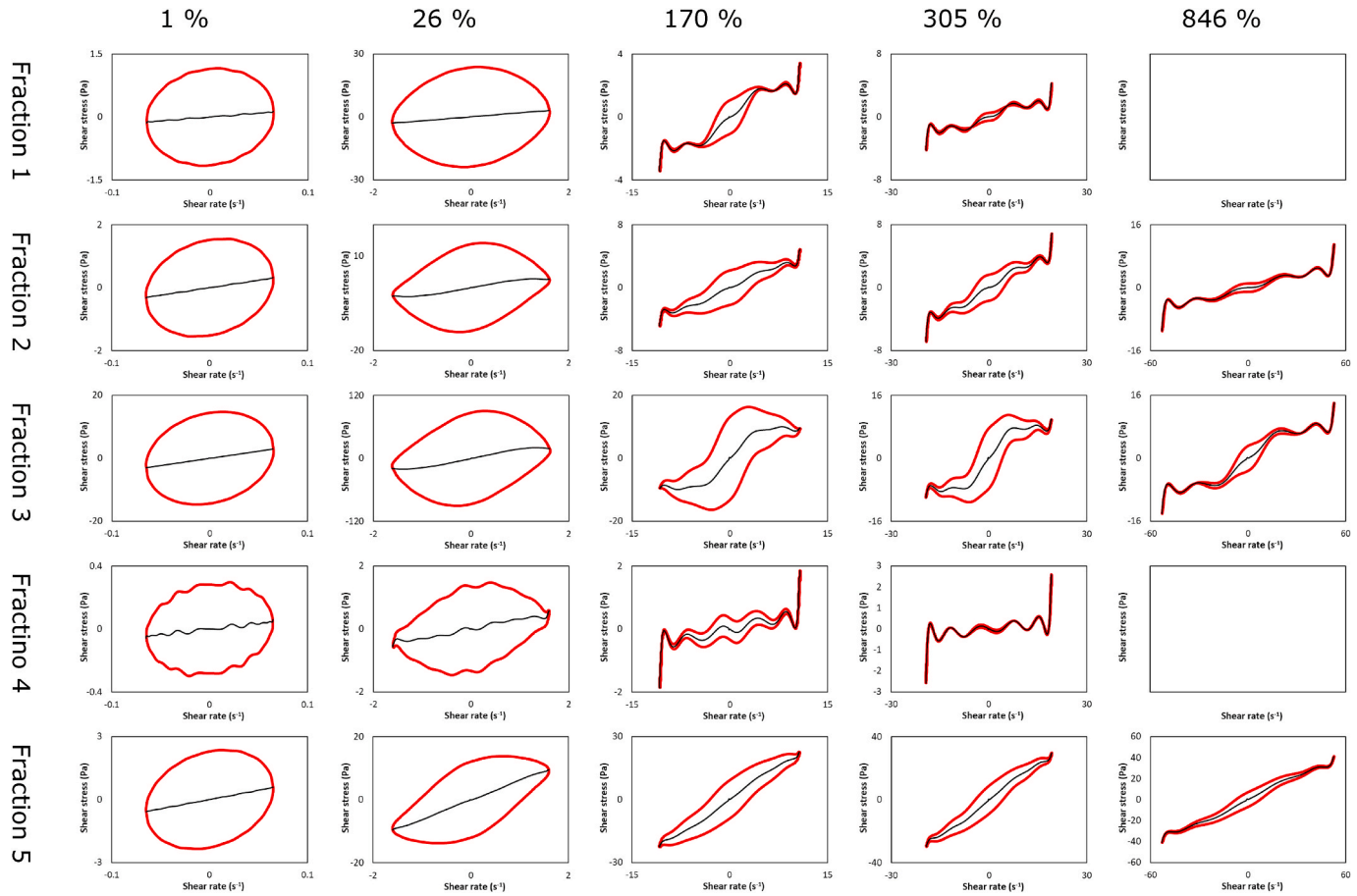

Fig. 4b. Lissajous plots of stress versus strain rate ($\tau,\dot{\gamma}$) at strains of 1, 26, 170, 305 and 846% for gelled fractions 1–5 (15 wt % d.m., pH 7). The black line represents the viscous stress contribution.

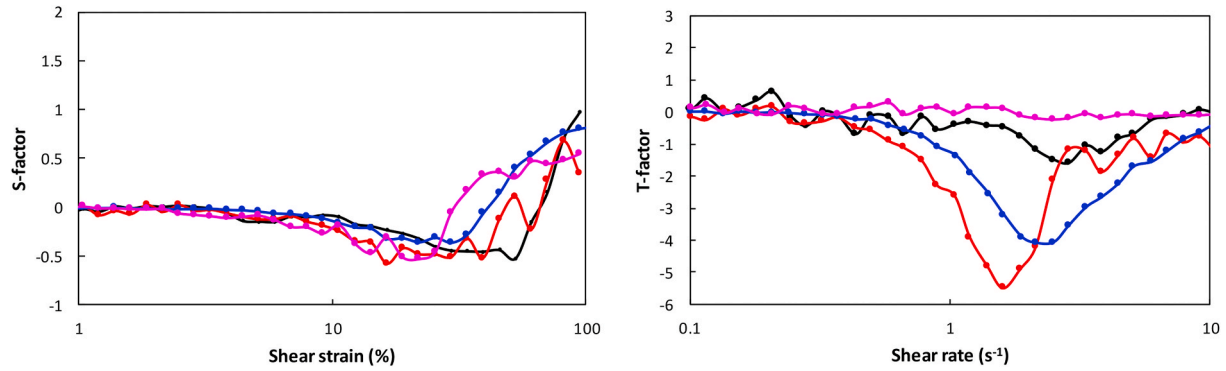

Fig. 5. Ratio of shear stiffening (S-factor) (left) and ratio of shear thickening (T-factor) (right) for the yellow pea fractions 1(▬),2(▬),3(▬) and 5 (▬) standardized on 15 wt % dry matter ad measured at pH 7. (For interpretation of the references to colour in this figure legend, the reader is referred to the Web version of this article.)

The viscous behaviour of the yellow pea fractions is shown in Fig. 4b. The shapes of the plots corresponding to fractions 2, 3 and 5 changed from a circular-shape to a rhomboidal-shape at low strain (26%), reflecting a transition from elastic to viscous dominated behaviour. At higher deformation the signal again showed strong oscillations, due to extreme nonlinearity and the presence of higher harmonics.

Fig. 5 shows that S < 0 ($G_L^{'} < G_M^{'}$) within a large strain region, indicating an overall mild strain softening behaviour for all fractions. The right panel of this figure shows stronger shear thinning behaviour (T < 0) for fraction 2 and 3, mild shear thinning behaviour for fraction 1 and no shear thinning behaviour for fraction 5. The absolute value of the T-factor is much higher than that of the S-factor, indicating an overall response of shear thinning for fraction 1–3. Fraction 5 is denser in protein than fraction 2 and 3 and it shows an earlier transition from elastic to viscous behaviour at large deformation. It seems that fraction 5 leads to a dense but weakly interacted network, whereas the limited processed fractions 2 and 3 leads to a firmer, cohesive and more stretchable system at large deformation.

Table 4
The protein-rich fractions from batches of different fractionation processes (n = 3) were averaged on their protein recovery and elastic moduli after heating. All gels were measured with 15 wt % pea fraction solubilized in deionized water at pH 7. The numbers in superscript represent the standard deviations and the different letters represent significant differences.

	Fraction 2	Fraction 3	Fraction 5
Recovery (%)	59 $^{\pm 9.8}$	74 $^{\pm 3.2}$	52.4 $^{\pm 7.3}$
G' (Pa)	756 $^{\pm 424\ a}$	1565 $^{\pm 751\ b}$	518 $^{\pm 144\ a}$

3.1.4. *Reproducibility of the fractionation processes and resulting observations*

For consistency reasons nearly all experiments were done with pea fractions originating from the same batch. Those results are representative of results that were observed for other batches. In order to strengthen our main statement that limited pea fractionation yields firmer gels per mass of protein at pH 7, we show the average and standard deviations of different batches regarding protein recovery and gel firmness. The results from different fractionation processes (n = 3) are compared for the protein-rich fractions 2, 3 and 5. Table 4 shows the protein recovery based on the separate fractionation processes. It also shows the average elastic moduli of the gelled fractions that originated from the different batches with a total number of at least seven measurements. The protein recovery and G' observed for the batch used in this study, as shown in Tables 1 and 3, are consistent with the average numbers shown in Table 4.

3.2. *Microstructure*

Fig. 6 shows CLSM images of the gels with the stained proteins shown in red. Fraction 1 seems to form a dense network at mesoscale, with large flour particles incorporated. The image indicates a continuous starch phase with protein distributed throughout. Fraction 2 and 3 show a somewhat discontinuous, but more homogeneous protein network at mesoscale. This is consistent with the rheological observations that indicated higher gel strength and strain softening behaviour. Fraction 4 shows a dispersion of protein aggregates combined with some non-protein material. The extensively processed fraction 5 shows a more heterogenous network with protein dense regions, indicated by a higher colour intensity in the CLSM images. Those regions are also seen in the electron microscopy images and could be caused by a higher protein content or by the presence of protein aggregates, as found in earlier research (Kornet et al., 2020).

CryoSEM was performed to further understand the microstructural properties and interactions of the starch-rich and protein-rich systems of fraction 1 and fraction 5 (Fig. 6). Energy-dispersive X-ray Spectroscopy (EDS) was used to obtain an elemental map of the imaged area, which is used to identify components based on their element density. The gelled

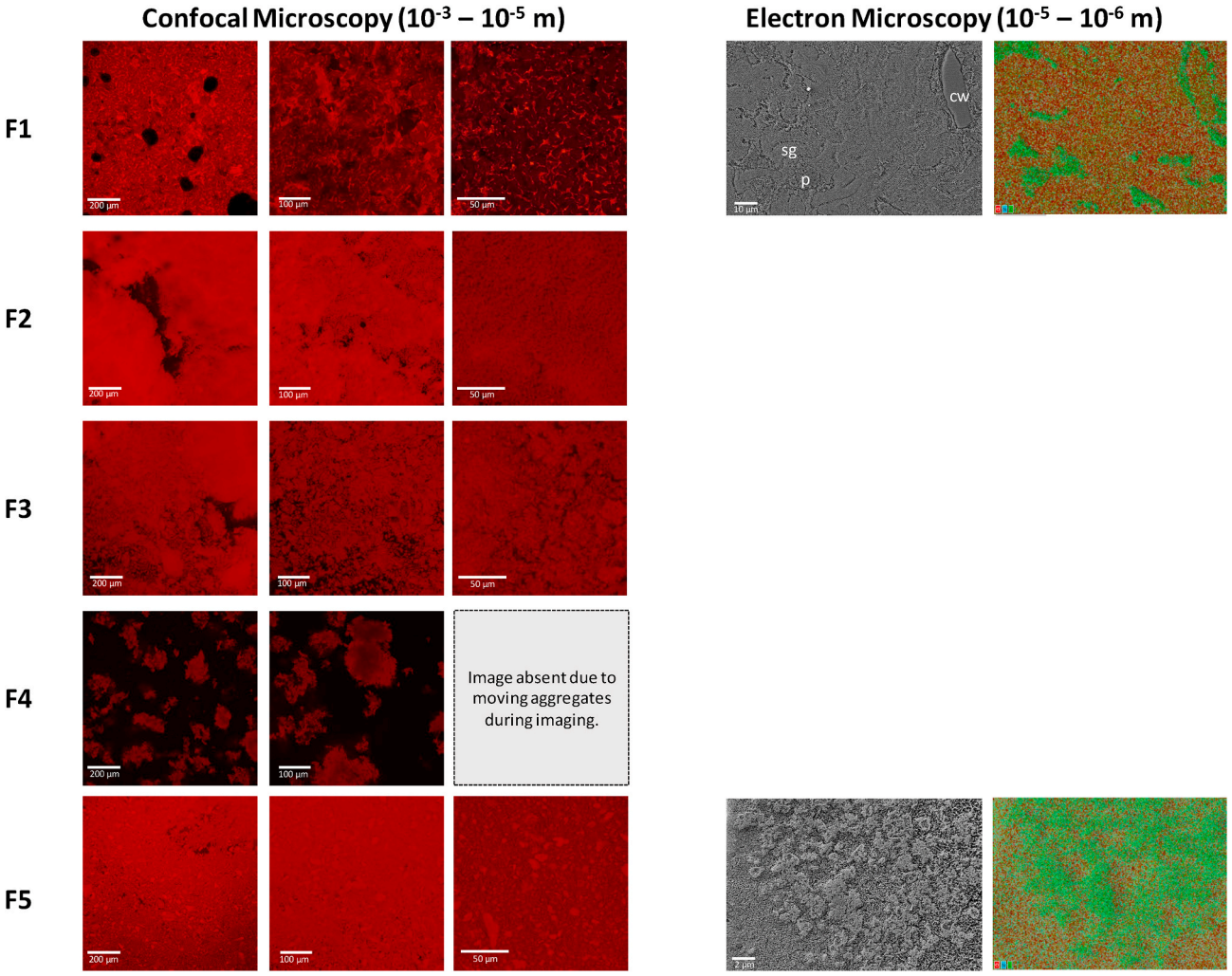

Fig. 6. CLSM images of gelled fraction 1–5 and CryoSEM images of gelled fractions 1 and 5 coupled with EDS, where red = oxygen, blue = nitrogen and green = carbon. sg = starch granule, p = protein, cw = cell wall material. All gels were made with 15 wt % pea fractions at pH 7. (For interpretation of the references to colour in this figure legend, the reader is referred to the Web version of this article.)

matrix was found to be heterogeneous with swollen starch granules, protein aggregates and a few oil droplets. Based on the elemental maps it was concluded that the continuous phase consisted of starch, substantiated by low nitrogen and denser oxygen and carbon. It is seen that the starch granules swell irregularly, fill the volume, leading to a dense starch system. Protein-dense regions are observed in between the starch granules and other cell components. The CryoSEM images are consistent with the assumption that starch is predominantly responsible for gelation in fraction 1.

The protein-rich fraction 5 was also visualized by CryoSEM, providing additional insight in the protein distribution in this heated paste-like system. The image shows protein-dense areas and EDS was used to confirm the presence of protein, showing indeed higher intensities of carbon and nitrogen. Pea protein in fractions 2, 3 and 5 were hypothesized in earlier work to be already in a partially aggregated state before heat treatment, as the protein was found to have a high volume to mass ratio (Kornet et al., 2020). The presence of more protein aggregates in fraction 5 than in fraction 2 and 3, could cause a lack of connectivity in the gelled matrix of fraction 5 and concomitant reduced gelling capacity due to the lower number of connections per unit volume that bare energy. We note however that this is not the only factor that is relevant to explain all observations as we will address from section 3.3 onwards.

3.3. Reduced gelling capacity upon fractionation

To understand why more extensive fractionation resulted in reduced gelling capacity per mass of protein at pH 7, different hypotheses were proposed and tested. The first set of tests were done to see whether impurities (i.e. sugars, salt, albumins) promoted the gelling capacity of fraction 2 and 3. The second set of tests were based on the suggestion that pH shifts in the fractionation process could result in irreversible changes in the protein structure, reducing their gelling capacity.

3.3.1. Ionic strength

One hypothesis was that differences in ionic strength, as indicated by differences in ash content (Table 1), could explain the reduced gelling capacity of fraction 5 compared to fractions 2 and 3. The elastic modulus G' after thermal treatment was measured at initial ionic strength, 20 mM NaCl and 200 mM NaCl addition. The G' of fraction 5 increased from $3.1*10^2$ to $1.4*10^3$ Pa and fractions 2 and 3 increased even less. Also at higher ionic strength fraction 5 does not significantly exceed the gel firmness of fractions 2 and 3, confirming the higher gelling capacity per mass of protein for fractions 2 and 3. To illustrate this, Fig. 7a shows the elastic moduli of fractions 2, 3 and 5 after standardization on an ionic strength of ~0.3 M. The finding of a higher gelling capacity per amount of protein for fractions 2 and 3 at standardized ionic strength, shows that the salt concentration has a relatively low influence.

3.3.2. Composition

In general, the composition itself had minor impact on the gelling capacity of the fractions. This is shown by reversing the fractionation by combining fraction 4 and 5 to yield a combined fraction with a composition of impurities and proteins equal to that of fraction 3. So, this combined fraction has the same composition as fraction 3, but its components have experienced a more severe processing due to the processing history of fraction 5. Fig. 7b shows that fraction 3 was significantly firmer than the combined fraction. This indicates that the fractionation processing alters the functionality of pea proteins. Interestingly, in this case the less severely processed fraction with a given composition exhibits a firmer gel than the fraction with the same composition but more severely processed, or, in other words, limited fractionation in this case implies a gel that is stronger. Following up on the importance of processing we look into the effect of lyophilization and isoelectric precipitation.

3.3.3. Lyophilization

It was hypothesized that the reduced gelling capacity of fraction 5 could be explained by a reduced thermal stabilization of sugars upon lyophilization. Table 1 shows that fraction 2 and 3 contain more carbohydrates than fraction 5 and from earlier research it is known that the vast majority of these carbohydrates are sugars (Kornet et al., 2020). Sugars can stabilize proteins upon lyophilization (Fedorov, Goodman, Nerukh, & Schumm, 2011). To verify the effect of freeze drying, fraction 2 was further purified with a 12.5 kDa membrane, to remove all sugars and salts, and its gelling capacity was compared to fraction 5 after lyophilization. Fig. 8a shows that, despite of the similar low sugar content, fraction 5 still had a significant lower elastic modulus ($9.2*10^2$ Pa) than the dialysed fraction 2 ($6.2 * 10^3$ Pa). This does not result in rejection of the hypothesis, but it is clear that the potential thermal stabilization cannot fully explain the differences between fractions 2 and 3 and fraction 5. Lyophilization probably has some effect on the protein state and functionality, but this again cannot fully explain the differences between fraction 2 and 3 and fraction 5.

3.3.4. pH changes and isoelectric precipitation

Another hypothesis was that pH changes or the isoelectric precipitation step is responsible for the reduced gelling capacity of fraction 5. Previous studies showed that pH changes can induce irreversible changes in soy and pea protein structure (Gueguen, Chevalier, & Schaeffer, 1988; Jiang et al., 2009). Although the pH changes applied in those studies were more extreme (i.e. < 3.5 and >9) than during the fractionation process (≥ 4.5 and ≤ 8), it was considered a plausible hypothesis, as even minor pH changes (i.e. pH 7–6) can have significant impact on the state of pea proteins (i.e. plant protein microcapsules) in dispersion (Cochereau, Nicolai, Chassenieux, & Silva, 2019). This

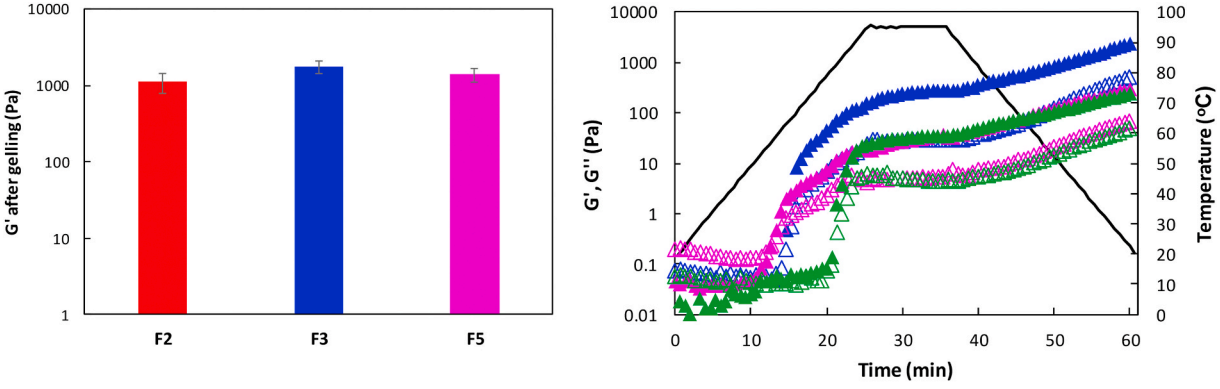

Fig. 7. The G' of fraction 2,3 and 5 at a standardized ionic strength of ~0.3 M with the error bars indicating the standard deviation (a) and comparison of fraction 3 and 5 with a mixture of fraction 4 and 5 to mimic fraction 3 (b). 3(▲), 5(▲) and 4/5 mixed (▲). All gels were made with 15 wt % pea fractions at pH 7. G': closed symbol and G'': open symbol.

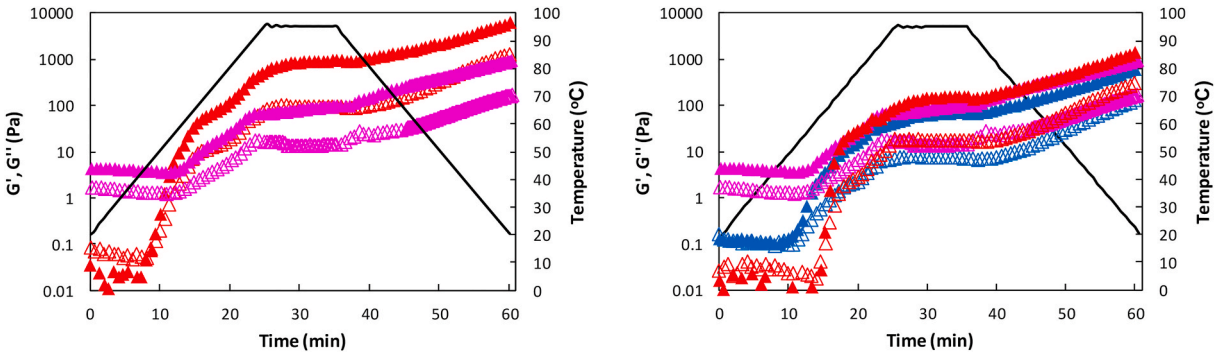

Fig. 8. The viscoelastic response of dialysed fraction 2 (▲) and fraction 5 (▲) (a) and comparison between fraction 2 (▲) and fraction 2 exposed to a pH shift (▲), fraction 5 (▲) is added as a reference (b). All gels were made with 15 wt % pea fractions at pH 7. *G'*: closed symbol and G": open symbol.

hypothesis was tested in two different ways, of which the results are shown in Fig. 8a and b. Fig. 8a shows a comparison between the precipitated fraction 5 and the non-precipitated (i.e. dialysed) fraction 2. It shows that replacement of a protein precipitation step by dialysis, yields a pea protein isolate (84 wt % protein) that has significantly ($P < 0.05$) higher G' after thermal treatment than the precipitated fraction 5 (87 wt % protein). This implies that isoelectric precipitation affects the gelling capacity of pea protein. Fig. 8b shows the sole effect of a pH change (7–4.5 and back to 7) on the gelling capacity of pea protein. Fraction 2 with and without pH shift are compared and a reduction of the eventual G' is observed ($1.4 * 10^3$ to $6.0 * 10^2$ Pa). This difference turned out to be insignificant ($P > 0.05$) when taking into account the average G' (756 Pa) observed for fraction 2, as shown in Table 4. In the pellet after centrifugation proteins are highly concentrated and around their isoelectric point, which may induce (irreversible) formation of protein aggregates. Based on the results from Fig. 8 we conclude that isoelectric precipitation can reduce the gelling capacity of pea protein.

3.3.5. *Pre-aggregation and interactions upon heating*

In earlier research it was found that pea proteins form aggregates with a low-density structure, which was also reflected in their average particle size (Table 5). The average particle size (350 nm) of fraction 5 is larger than that of fraction 2 and 3 (94 and 242 nm respectively). Those numbers originate from dynamic light scattering measurements and the corresponding particle size distributions indicated polydispersity (Kornet et al., 2020). These size distributions are obtained as a plot of the relative intensity of the light scattered by the particles in the various size classes.

Although there is a reduction in exposed thiol groups after heating the fractions (Table 5), S–S bonding does not play an active role in the heat-induced gelation process (Sun et al., 2012). This was also confirmed by an additional experiment with the thiol-blocking agent NEM on fractions 3 and 5. The incubated samples showed similar gelling behaviour upon heating as the non-incubated ones (not shown here). The observed reduction in exposed thiol groups could mean that upon heating there is S–S bonding to some extent, but it does not greatly affect the eventual network structure. Another possibility is that fever thiol groups were detected, not because they formed S–S bonds, but simply because they were buried in the protein aggregates after heating. Furthermore, it has been reported for pea proteins that hydrophobic interactions and hydrogen bonding are mainly responsible for heat-induced gelation (Sun et al., 2012). However, differences in relative hydrophobicity, as shown in Table 5, could not explain differences in gelling behaviour. To exclude the effect of electrostatic interactions, the electrophoretic mobility was measured and is shown in Table 5. The values indicate that the average charges of all dispersed fractions are at pH 7. This means that in the measured systems there is electrostatic repulsion that prevents the proteins from interacting at room temperature and influences the rate and extent of gelation upon heating. As the ζ-potentials are of a similar order of magnitude, it cannot explain the differences in gelling capacity observed for the different fractions.

4. Conclusion

In this study we linked the extent of aqueous fractionation on the gelling capacity, defined as the capacity per mass of protein to increase the *G'* after thermal treatment, and linear and non-linear gel properties of the resulting fractions. SAOS rheology showed that limited fractionation yields higher protein gelling capacity. Gelation of pea flour was mainly caused by starch gelatinization, whereas the gelation of protein-enriched fractions was caused by interacting proteins. Limited processed fractions were found to form firmer gels with strain softening behaviour. The more extensively fractionated sample was less firm and showed an earlier transition to viscous behaviour at large deformation, indicating a weakly interacting network. Microstructure images were consistent with these observations. A number of experiments, involving changes in the extraction process and rheological measurements, indicated that the reducing gelling capacity upon fractionation is caused by a combination of factors, which are isoelectric precipitation, amount of sugars upon lyophilization and differences in ash content. All three factors would unequivocally decrease the gelling capacity upon fractionation. In conclusion, limited fractionation in the case of pea protein leads to a higher gelling capacity and stronger gels per mass of protein.

From a scientific perspective, the outcome of this study could be

Table 5
An overview of the physical properties of fractions 1–5 at pH 7 and I < 0.1 M NaCl equivalent. The type of proteins and average particle size was determined by Kornet et al., 2020. The number of sulfhydryl groups per gram of protein is determined before and after heating and was measured at pH 8. Standard deviations or R^2 for hydrophobicity are displayed in superscript.

Pea fraction	Type of proteins	Average particle size (nm)	Relative hydrophobicity (Arb. Unit)*	Thiol groups (μmol SH-groups/g protein)	ζ-potential (mV)
Fraction 1	Both	ND	$6.6^{0.99}$	$32.2^{\pm0.4}$ | $46.3^{\pm0.1}$	$-23.4^{\pm1.1}$
Fraction 2	Both	$94^{\pm3}$	$6.7^{0.95}$	$55.6^{\pm0.2}$ | $33.7^{\pm0.0}$	$-20.7^{\pm1.8}$
Fraction 3	Both	$242^{\pm4}$	$9.5^{0.98}$	$52.3^{\pm0.7}$ | $39.5^{\pm0.1}$	$-23.3^{\pm1.0}$
Fraction 4	Albumins	$110^{\pm14}$	$\ll 1$	$168^{\pm3.3}$ | $138^{\pm0.7}$	$-15.1^{\pm1.2}$
Fraction 5	Globulins	$350^{\pm8}$	$9.5^{0.97}$	$49.6^{\pm1.9}$ | $43.9^{\pm0.8}$	$-24.7^{\pm1.2}$

taken further by systematically exploring the effect of concentration, pH and ionic strength on the gelling capacity of the pea fractions. Furthermore, future research could focus on characterizing the gels by varying the frequency in LAOS experiments and studying the gel recovery behaviour by applying multiple strain sweeps. From an industrial perspective, our research and future research could help optimizing their fractionation processes in view of sustainability and ingredient functionality.

CRediT authorship contribution statement

Remco Kornet: Conceptualization, Formal analysis, Data curation, Methodology, Investigation, Writing - original draft, Visualization. **Justus Veenemans:** Investigation, Validation, Data curation. **Paul Venema:** Supervision, Methodology, Conceptualization, Writing - review & editing. **Atze Jan van der Goot:** Conceptualization, Writing - review & editing. **Marcel Meinders:** Funding acquisition, Project administration, Writing - review & editing. **Leonard Sagis:** Formal analysis, Writing - review & editing. **Erik van der Linden:** Project administration, Funding acquisition, Supervision, Writing - review & editing.

Declaration of competing interest

The authors have declared that no competing interests exist.

Acknowledgements

The authors thank Jaap Nijsse and Caroline Remijn for electron microscopy. They also thank Stephan Schumm for pointing out that sugars can stabilize proteins upon lyophilization, giving rise to one of the hypotheses that we tested. Remco Kornet thanks Xilong Zhou for fruitful discussions about rheology in general. The project is organised by and executed under the auspices of TiFN, a public - private partnership on precompetitive research in food and nutrition. The authors have declared that no competing interests exist in the writing of this publication. Funding for this research was obtained from Unilever Research and Development Nutricia Research B·V., Fromageries Bel S. A., Pepsico Inc., and the Top sector Agri&Food.

References

Bandyopadhyay, R., Liang, D., Harden, J. L., & Leheny, R. L. (2006). Slow dynamics, aging, and glassy rheology in soft and living matter. *Solid State Communications, 139*(11–12), 589–598.

Berghout, J. A. M., Venema, P., Boom, R. M., & van der Goot, A. J. (2015). Comparing functional properties of concentrated protein isolates with freeze-dried protein isolates from lupin seeds. *Food Hydrocolloids, 51*, 346–354.

Biliaderis, C., Maurice, T., & Vose, J. (1980). Starch gelatinization phenomena studied by differential scanning calorimetry. *Journal of Food Science, 45*(6), 1669–1674.

Birbaum, F. C., Haavisto, S., Koponen, A., Windhab, E. J., & Fischer, P. (2016). Shear localisation in interfacial particle layers and its influence on Lissajous-plots. *Rheologica Acta, 55*(4), 267–278.

Cho, K. S., Hyun, K., Ahn, K. H., & Lee, S. J. (2005). A geometrical interpretation of large amplitude oscillatory shear response. *Journal of Rheology, 49*(3), 747–758.

Cochereau, R., Nicolai, T., Chassenieux, C., & Silva, J. V. (2019). Mechanism of the spontaneous formation of plant protein microcapsules in aqueous solution. *Colloids and Surfaces A: Physicochemical and Engineering Aspects, 562*, 213–219.

Creighton, T. E. (1997). *Protein structure: A practical approach*. IRL Press at Oxford University Press.

Duvarci, O. C., Yazar, G., & Kokini, J. L. (2017). The comparison of Laos behavior of structured food materials (suspensions, emulsions and elastic networks). *Trends in Food Science & Technology, 60*, 2–11.

Ellman, G. L. (1959). Tissue sulfhydryl groups. *Archives of Biochemistry and Biophysics, 82*(1), 70–77.

Ewoldt, R. H., Hosoi, A., & McKinley, G. H. (2008). New measures for characterizing nonlinear viscoelasticity in large amplitude oscillatory shear. *Journal of Rheology, 52*(6), 1427–1458.

Fedorov, M. V., Goodman, J. M., Nerukh, D., & Schumm, S. (2011). Self-assembly of trehalose molecules on a lysozyme surface: The broken glass hypothesis. *Physical Chemistry Chemical Physics, 13*(6), 2294–2299.

Fuhrmeister, H., & Meuser, F. (2003). Impact of processing on functional properties of protein products from wrinkled peas. *Journal of Food Engineering, 56*(2–3), 119–129.

Fuongfuchat, A., Seetapan, N., Makmoon, T., Pongjaruwat, W., Methacanon, P., & Gamonpilas, C. (2012). Linear and non-linear viscoelastic behaviors of crosslinked tapioca starch/polysaccharide systems. *Journal of Food Engineering, 109*(3), 571–578.

van der Goot, A. J., Pelgrom, P. J., Berghout, J. A., Geerts, M. E., Jankowiak, L., Hardt, N. A., et al. (2016). Concepts for further sustainable production of foods. *Journal of Food Engineering, 168*, 42–51.

ount(preceding-sibling::sb:reference[1])"?^(1)[ref_tag]>Gueguen, J., Chevalier, M., & Schaeffer, F. (1988). Dissociation and aggregation of pea legumin induced by pH and ionic strength. *Journal of the Science of Food and Agriculture, 44*(2), 167–182.

Jiang, J., Chen, J., & Xiong, Y. L. (2009). Structural and emulsifying properties of soy protein isolate subjected to acid and alkaline pH-shifting processes. *Journal of Agricultural and Food Chemistry, 57*(16), 7576–7583.

Kato, A., & Nakai, S. (1980). Hydrophobicity determined by a fluorescence probe method and its correlation with surface properties of proteins. *Biochimica et Biophysica Acta (BBA) - Protein Structure, 624*(1), 13–20.

Kornet, C., Venema, P., Nijsse, J., van der Linden, E., van der Goot, A. J., & Meinders, M. (2020). Yellow pea aqueous fractionation increases the specific volume fraction and viscosity of its dispersions. *Food Hydrocolloids, 99*, 105332.

Lam, A. C. Y., Can Karaca, A., Tyler, R. T., & Nickerson, M. T. (2016). Pea protein isolates: Structure, extraction, and functionality. *Food Reviews International*, 1–22.

Makri, E., Papalamprou, E., & Doxastakis, G. (2005). Study of functional properties of seed storage proteins from indigenous European legume crops (lupin, pea, broad bean) in admixture with polysaccharides. *Food Hydrocolloids, 19*(3), 583–594.

Mession, J.-L., Sok, N., Assifaoui, A., & Saurel, R.m. (2013). Thermal denaturation of pea globulins (pisum sativum L.) molecular interactions leading to heat-induced protein aggregation. *Journal of Agricultural and Food Chemistry, 61*(6), 1196–1204.

Ntone, E., Bitter, J. H., & Nikiforidis, C. V. (2020). Not sequentially but simultaneously: Facile extraction of proteins and oleosomes from oilseeds. *Food Hydrocolloids, 102*, 105598.

O'Kane, F. E. (2004). *Molecular characterisation and heat-induced gelation of pea vicilin and legumin*.

O'Kane, F. E., Happe, R. P., Vereijken, J. M., Gruppen, H., & van Boekel, M. A. (2004). Heat-induced gelation of pea legumin: Comparison with soybean glycinin. *Journal of Agricultural and Food Chemistry, 52*(16), 5071–5078.

Papalamprou, E., Doxastakis, G., Biliaderis, C., & Kiosseoglou, V. (2009). Influence of preparation methods on physicochemical and gelation properties of chickpea protein isolates. *Food Hydrocolloids, 23*(2), 337–343.

Precha-Atsawanan, S., Uttapap, D., & Sagis, L. M. (2018). Linear and nonlinear rheological behavior of native and debranched waxy rice starch gels. *Food Hydrocolloids, 85*, 1–9.

Puppo, M., Beaumal, V., Speroni, F., De Lamballerie, M., Añón, M., & Anton, M. (2011). β-Conglycinin and glycinin soybean protein emulsions treated by combined temperature–high-pressure treatment. *Food Hydrocolloids, 25*(3), 389–397.

Ratnayake, W. S., Hoover, R., & Warkentin, T. (2002). Pea starch: Composition, structure and properties—a review. *Starch Staerke, 54*(6), 217–234.

Schutyser, M. A. I., Pelgrom, P. J. M., van der Goot, A. J., & Boom, R. M. (2015). Dry fractionation for sustainable production of functional legume protein concentrates. *Trends in Food Science & Technology, 45*(2), 327–335.

Shand, P. J., Ya, H., Pietrasik, Z., & Wanasundara, P. K. J. P. D. (2007). Physicochemical and textural properties of heat-induced pea protein isolate gels. *Food Chemistry, 102*(4), 1119–1130.

Sridharan, S., Meinders, M. B., Bitter, J. H., & Nikiforidis, C. V. (2020). Pea flour as stabilizer of oil-in-water emulsions: Protein purification unnecessary. *Food Hydrocolloids, 101*, 105533.

Stone, A. K., Karalash, A., Tyler, R. T., Warkentin, T. D., & Nickerson, M. T. (2015). Functional attributes of pea protein isolates prepared using different extraction methods and cultivars. *Food Research International, 76*, 31–38.

Sun, X. D., & Arntfield, S. D. (2010). Gelation properties of salt-extracted pea protein induced by heat treatment. *Food Research International, 43*(2), 509–515.

Sun, X. D., & Arntfield, S. D. (2011). Gelation properties of salt-extracted pea protein isolate induced by heat treatment: Effect of heating and cooling rate. *Food Chemistry, 124*(3), 1011–1016.

Sun, X. D., & Arntfield, S. D. (2012). Molecular forces involved in heat-induced pea protein gelation: Effects of various reagents on the rheological properties of salt-extracted pea protein gels. *Food Hydrocolloids, 28*(2), 325–332.

Taherian, A. R., Mondor, M., Labranche, J., Drolet, H., Ippersiel, D., & Lamarche, F. (2011). Comparative study of functional properties of commercial and membrane processed yellow pea protein isolates. *Food Research International, 44*(8), 2505–2514.

Wierenga, P. A., Kosters, H., Egmond, M. R., Voragen, A. G., & de Jongh, H. H. (2006). Importance of physical vs. chemical interactions in surface shear rheology. *Advances in Colloid and Interface Science, 119*(2–3), 131–139.

Yazar, G., Duvarci, O., Tavman, S., & Kokini, J. L. (2017). Non-linear rheological behavior of gluten-free flour doughs and correlations of Laos parameters with gluten-free bread properties. *Journal of Cereal Science, 74*, 28–36.